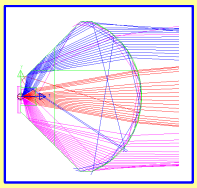

Ventura Photonics

Photonics Solutions

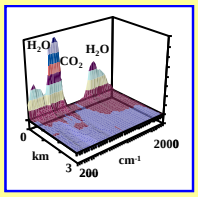

What Do We Mean By Surface Temperature?

Roy Clark PhD

Ventura Photonics Climate Note 4, VPCN 004.1
Thousand Oaks, CA
September 2019

The term 'surface temperature' has a variety of meanings. Logically, it should refer to the temperature at the earth's air-surface interface. However, it is often taken to mean the weather station temperature. This is not a surface temperature. Instead, it is the meteorological surface air temperature (MSAT). This is the temperature measured by a thermometer installed in a ventilated enclosure located for convenience near eye level, 1.5 to 2 m above the ground [Oke, 2016]. Historically in the US, the daily minimum and maximum MSATs were recorded using Six's thermometer. The min and max readings are often averaged to give an 'average daily temperature'.

The climate record is not simply the long term average of the weather station data [Andrews, 2017a; 2017b; 2017c; D'Aleo, 2010]. First, the raw data is processed using 'homogenization' to remove measurement 'bias' and 'infilling' to create values for missing data. Area weighted averages within given latitude and longitude 'bins' are then determined. To compare the weather station record to computer model predictions, the 'temperature anomaly' is often used. This is the long term temperature record with the mean subtracted to highlight the trends. The mean is usually taken over a 30 year reference period. The apparent trends can depend on how the reference period is selected. The end result may bear little resemblance to the raw data. These climate data sets are then analyzed using advanced mathematical techniques to find trends that may or may not be real. To the analyst, the data set is often just a number series, completely disconnected from the original temperature measurements and devoid of any physical meaning.

The climate models do not use any kind of thermal engineering analysis to determine the surface temperature. Instead, the models use an approach known as radiative forcing. It is well known that an increase in surface temperature will produce an increase in the outgoing long wave radiation (OLR) at the top of the atmosphere (TOA) or the tropopause. The OLR response to the surface temperature is approximately linear [Koll and Cronin, 2018]. Radiative forcing assumes that this energy transfer process works in reverse. A calculated change in long wave IR (LWIR) flux at the TOA or the tropopause somehow produces a change in 'equilibrium surface temperature'. The radiative forcing calculation used to convert the change in LWIR flux to a temperature is a

prescribed mathematical ritual that has changed little since it was described by Hansen et al in 1981 [[IPCC Ch.8, 2013; Hansen et al, 2005; 1981]. This approach assumes that some kind of average equilibrium climate state exists. Then it is assumed that an increase in atmospheric CO_2 concentration will perturb this equilibrium state and produce a new state with a higher surface temperature.

In reality, there is no such thing as an average equilibrium climate. The surface temperature is determined by the energy transfer processes at the surface, including thermal storage. Furthermore, the time dependence must be included. The local solar flux is always changing on a daily and a seasonal time scale. At night it is zero. The concept of a 24 hour average solar flux has little useful meaning. The starting point for any analysis of the surface temperature is that the solar heat absorbed by the surface is stored in a thermal reservoir. Any change in temperature is determined by the change in the heat content or enthalpy contained in the reservoir divided by the heat capacity [Clark, 2019a; b; Clark, 2013a, b]. For non-equilibrium conditions, the coupled LWIR flux defines a rate of heating or cooling, not an equilibrium temperature. The LWIR flux cannot be separated from the other flux terms including the solar flux, the convective or sensible heat flux, the evaporative or latent heat flux and subsurface conduction on land or the convective circulation and transport in the oceans. The air-land and air-ocean interfaces have different energy transfer properties and need to be considered separately.

Over land, all of the flux terms are coupled into a thin surface layer. This layer is heated during the day by the absorbed solar flux. The net LWIR emission from the surface is insufficient to remove the surface heat. Instead, the land warms up until the heat is dissipated by moist convection. The warm land surface establishes a thermal gradient with both the cooler air above and the subsurface ground layers below. For a dry surface under full tropical or summer sun illumination, the surface temperature may reach or exceed 50 C, with a thermal gradient of approximately 20 C. Here the surface-air thermal gradient is taken as the difference between the surface and the MSAT temperatures. Other definitions may be used. The air is heated by direct thermal transfer from the warmer surface. This establishes an upward convective cooling air flow or sensible heat flux from the surface. If the surface is moist, evaporation also occurs and the latent heat flux reduces the temperature rise. The subsurface thermal gradient conducts heat below the surface during the first part of the day. Later, as the solar flux decreases, the thermal gradient reverses and the stored subsurface heat is returned to the surface. The energy transfer processes at the air-land interface are illustrated in Figure 1.

The maximum and minimum MSATs measure temperatures that are produced by two very different energy transfer processes. The minimum MSAT generally occurs near dawn. At this time, the surface air layer and the ground are usually at similar temperatures and the minimum MSAT is approximately that of the bulk surface air temperature of the local weather system that is passing through. The maximum MSAT is generally recorded in the early afternoon after the peak solar flux at local noon. It is the air temperature produced by the convective mixing of the warm air rising from the surface as it interacts with the cooler air at the MSAT thermometer level. The increase in temperature from the minimum to the maximum is a combined measure of

convective mixing, solar flux, cloud cover and surface moisture/precipitation. This mean that the energy transfer information is contained in the minimum MSAT and the delta or (max – min) MSAT.

An important concept here is the convection transition temperature. During the late afternoon or evening, the land cools until it approaches the surface air temperature. There is no longer a thermal gradient to drive the convection so the surface now cools more slowly by net LWIR emission. This continues through the night until the surface is heated again by the sun the following day. The convection transition temperature at which the surface and air temperatures equalize depends on the bulk air temperature of the local weather system. This is reset each day by the local weather patterns.

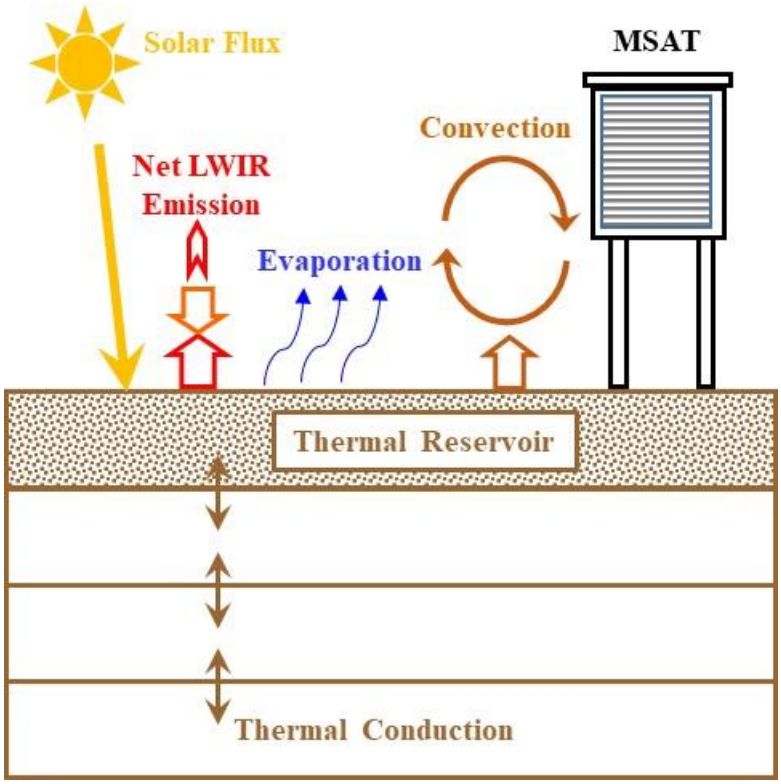

Figure 1: Energy transfer processes at the air-land interface.

Over the ocean, the surface is almost transparent to the solar flux. Approximately half of this flux is absorbed within the first meter layer of the ocean and 90% is absorbed within the first 10 m layer. The thermal gradient at the air-ocean interface is much small than that at the air-land surface. Typically it is only 1 or 2 C. This means that the absorbed solar flux cannot be dissipated by the combined net LWIR and sensible heat flux. The ocean surface must warm up until the excess heat is removed by the latent heat from wind driven surface evaporation. The cooler water produced at the surface then sinks and cools the bulk ocean layers below. It is replaced by upwelling warm water. This is a Rayleigh-Benard type of convection with columns of water moving in opposite directions. It is not a simple diffusion process. This convection cycle continues to provide heat to

the surface at night, so the wind driven evaporation continues at night. The thermal storage is not localized and heat can be transported and recirculated over very long distances. The penetration depth of the LWIR flux into the ocean surface is 100 μm or less. Evaporation involves the removal of water molecules from the surface. These two processes are combined within the first 100 μm layer and cannot be separated. The energy transfer processes at the air-ocean interface are illustrated in Figure 2.

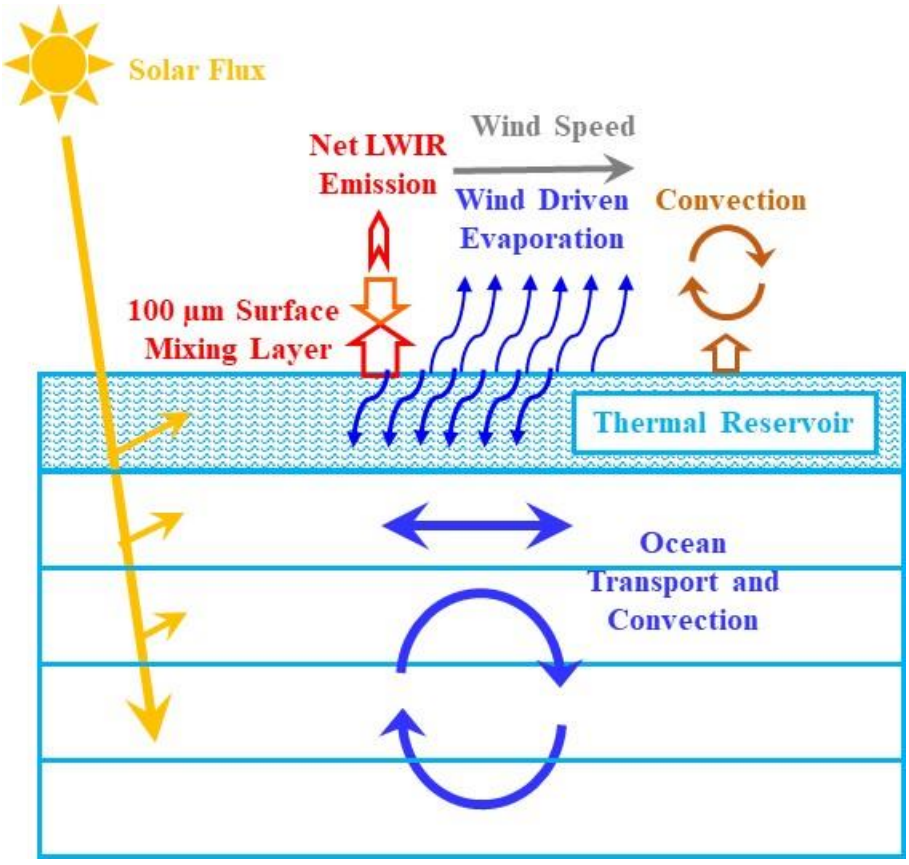

Figure 2: Energy transfer processes at the air-ocean interface.

An important concept related to the time dependence that is lost in the temperature averaging is the time delay or phase shift between the peak solar flux and the temperature response. There are four different time delays or phase shifts that occur at the land-air interface. First, there is the delay between the solar flux and the surface temperature response. Second, there is the delay between the surface temperature response and the air temperature change. These two are coupled since an increase in air temperature also leads to an increase in the LWIR exchange energy and a change in convective flux. Third there is the delay between the surface temperature response and the subsurface temperature change. This delay increases with depth. It was described by Fourier in 1827 [Fourier, 1827]. Fourth, there is a seasonal delay between the solstice/equinox points and the surface temperature response. This seasonal delay is a result of dynamic ocean thermal storage. It is transported by the various weather systems and coupled to the land surface via the convection

transition temperature. Selected examples of the various land surface phase shifts are shown in Figures 3a through 3d.

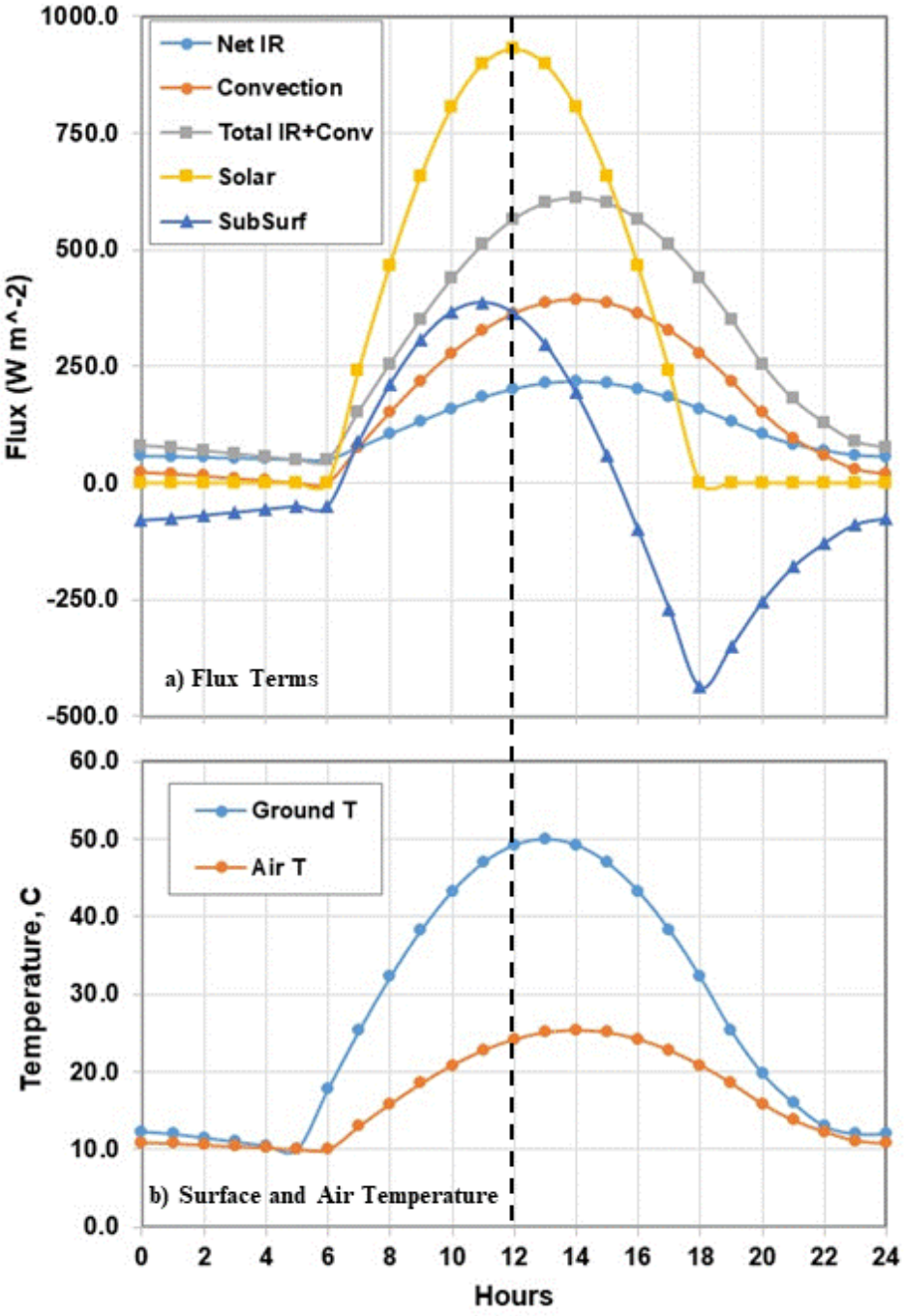

a) Flux terms and b) surface and air temperatures for a dry surface under full summer sun illumination conditions. Derived from UC Irvine 'Grasslands' data.

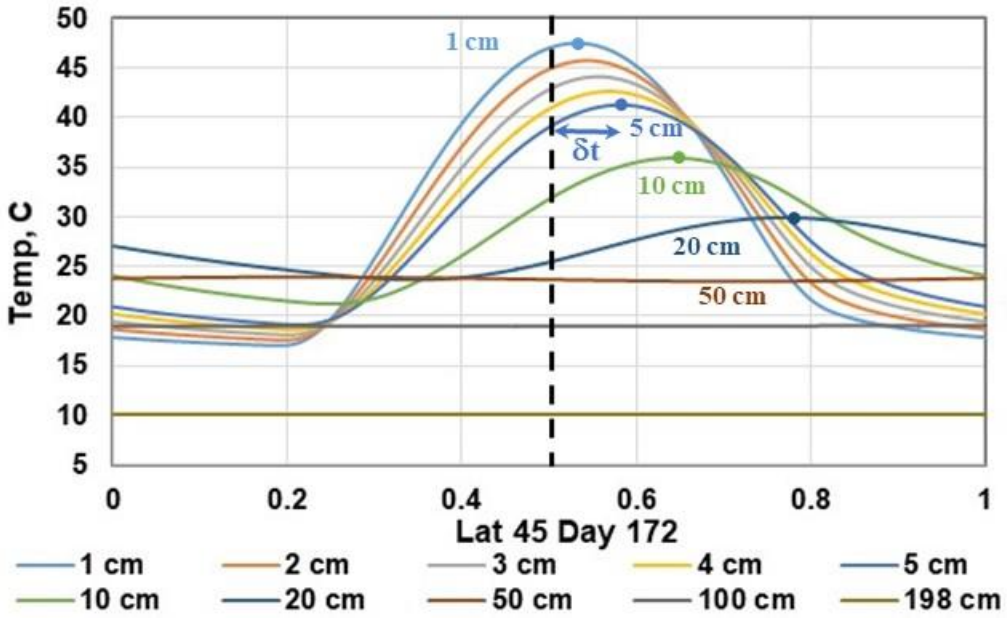

c) Subsurface heating: the phase shift or time delay for the temperature response increases with depth. The magnitude of the heating decreases with depth and is limited in this example to the first 50 cm layer.

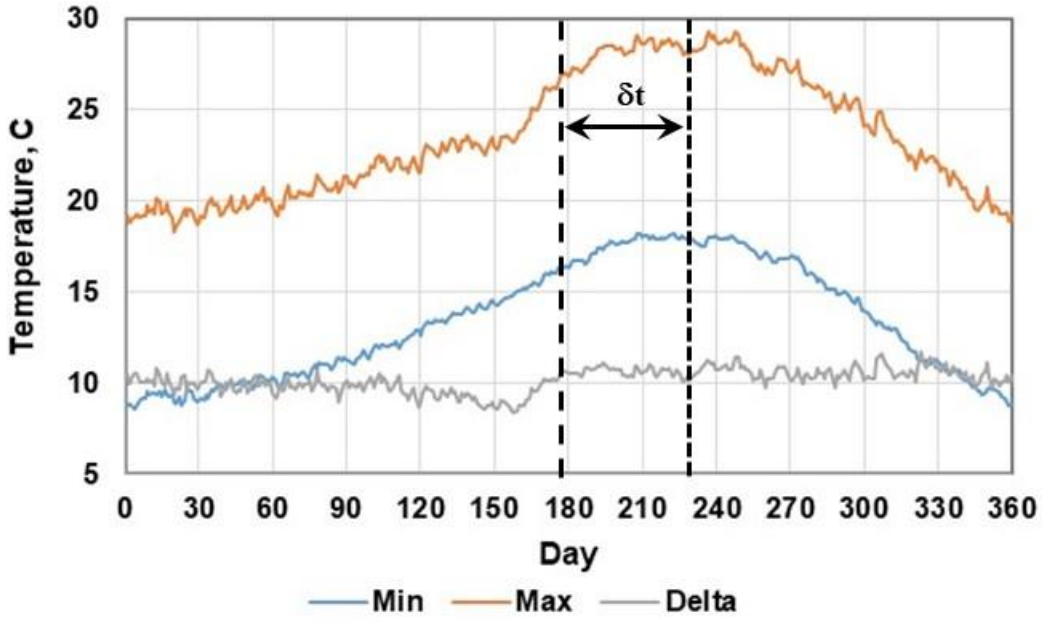

d) Daily average min, max and delta MSAT for Los Angeles civic Center, 1922 to 2008. The delta T stays near 10 C for the whole year.

Figure 3: Phase shift and temperature data: a) diurnal surface flux terms and b) surface and air temperatures for a dry surface under full summer sun illumination, c) Calculated subsurface temperatures for dry surface, full summer sun illumination, 45 latitude. d) Daily average min, max and delta MSAT for Los Angeles Civic Center showing the seasonal phase shift.

Over the oceans there is a diurnal phase shift between the solar flux and the ocean surface temperature rise that depends on both the solar flux and the wind speed. Figure 4 shows the effect of wind speed on the diurnal temperature rise recorded at the TRITON buoy located on the equator at a longitude of 165° E in the Pacific warm pool. These data were recorded during July 2010 [Clark, 2013b].

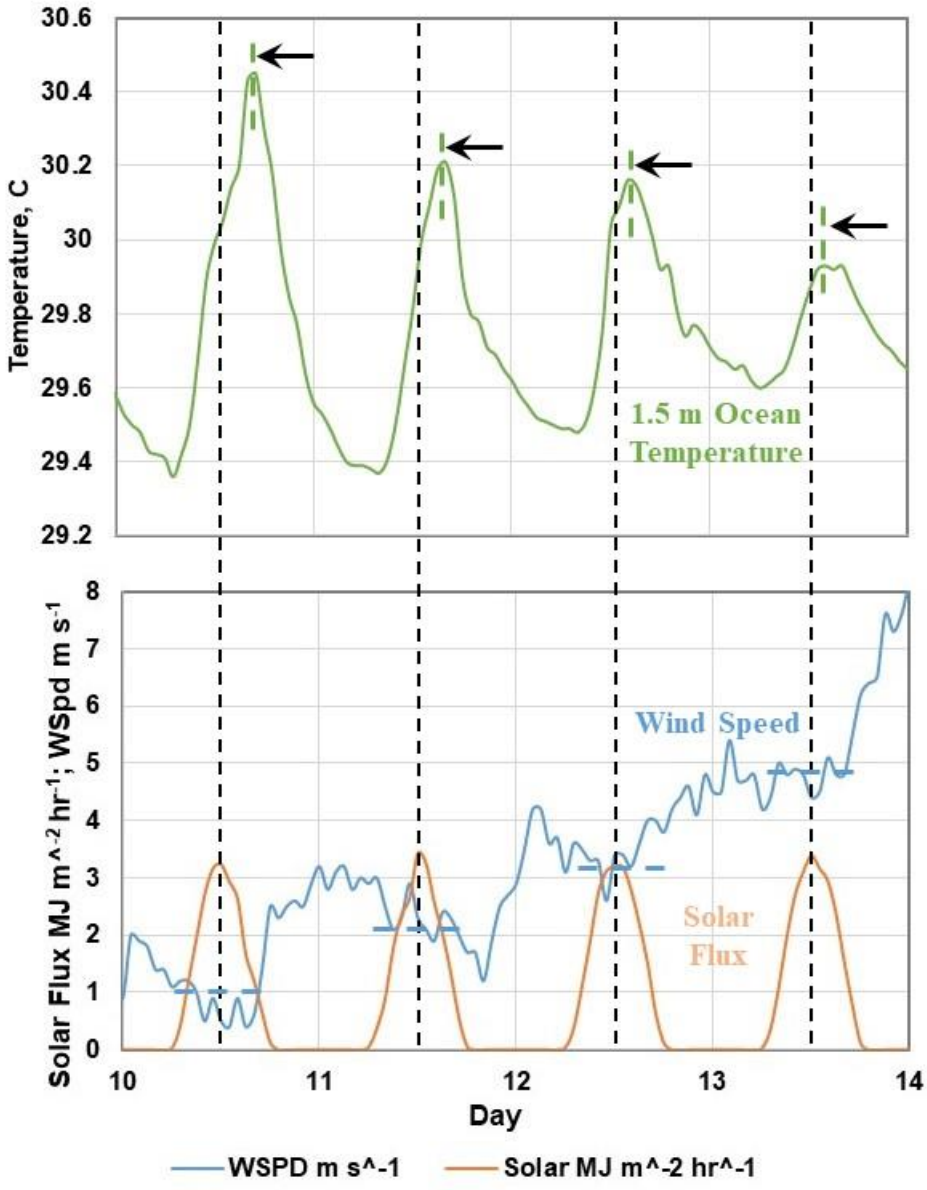

Figure 4: 1.5 m ocean temperature, wind speed and solar flux for 4 days, July 2010 recorded at the TRITON buoy on the equator at 165 E in the Pacific warm pool. The diurnal temperature rise and the magnitude of the phase shift decrease with increasing wind speed.

During the summer at most latitudes, the solar heating exceeds the wind driven cooling. The lower ocean subsurface layers are not coupled to the surface by convective mixing and a stable thermal gradient is established. During the winter, the wind driven evaporation exceeds the solar heating and the surface temperatures cool and establish a uniform temperature layer down to 100 m or lower. There is a significant time relay or phase shift of 4 to 8 weeks between the solstice and the ocean max/min temperature response. Figure 5 shows the seasonal variation in ocean temperature at nominal depths of 5, 25, 50, 75 and 100 m derived from Argo float data [Clark, 2013a, 2013b]. Figure 5a shows the temperature data from a float drifting in the S. Pacific Ocean at latitudes and longitudes near 21° S and 105° W. Higher latitudes show a similar behavior with lower temperatures because of reduced solar heating.

At low latitudes near the equator, the diurnal and seasonal temperature variations may not be sufficient to mix the subsurface layers below the 25 to 50 m levels and heat can accumulate at these depths for extended periods. Figure 5b shows the temperature data from an Argo float drifting in the S. Pacific Ocean at latitudes and longitudes near 1.5° S and 126° W. The diurnal mixing layer is shallow and only extends down to the 50 m level about half of the time. The floats are not tethered and the decrease in near-surface temperature with time is caused by an eastward drift.

Heat continues to accumulate as the ocean water travels westwards with the Pacific equatorial current. This leads to the formation of the equatorial ocean warm pool in the western Pacific Ocean. The ocean surface temperature increases until the wind driven evaporation balances the tropical solar heating at a surface temperature near 30 C and an average wind speed near 5 m s^{-1}. Variations in the wind speed across the Pacific Ocean then produce the characteristic El Nino Southern Oscillation (ENSO). As the wind speed slows, the evaporation decreases and the ocean current velocity decreases. Both of these factors increase the rate of surface heating and the warm pool extent increases.

The changes in ocean surface temperature produced by the ENSO and other ocean oscillations such as the Pacific decadal oscillation (PDO) and the Atlantic Multi-decadal Oscillation (AMO) are transported over long distances by the weather systems that form over the oceans. They are coupled into the weather station record through the daily convection transition temperature. The seasonal ocean phase shift may therefore be found in weather station records far inland. Figure 6 shows the 30 year climate daily average minimum and maximum temperatures for selected weather stations at 34°, 45° and 20° latitudes. The dotted lines indicate the peak solar flux at summer solstice. The seasonal phase shifts can be seen in the peak temperatures that occur after solstice [Clark, 2019a]. The 45° data include Sioux Falls and Flandreau SD.

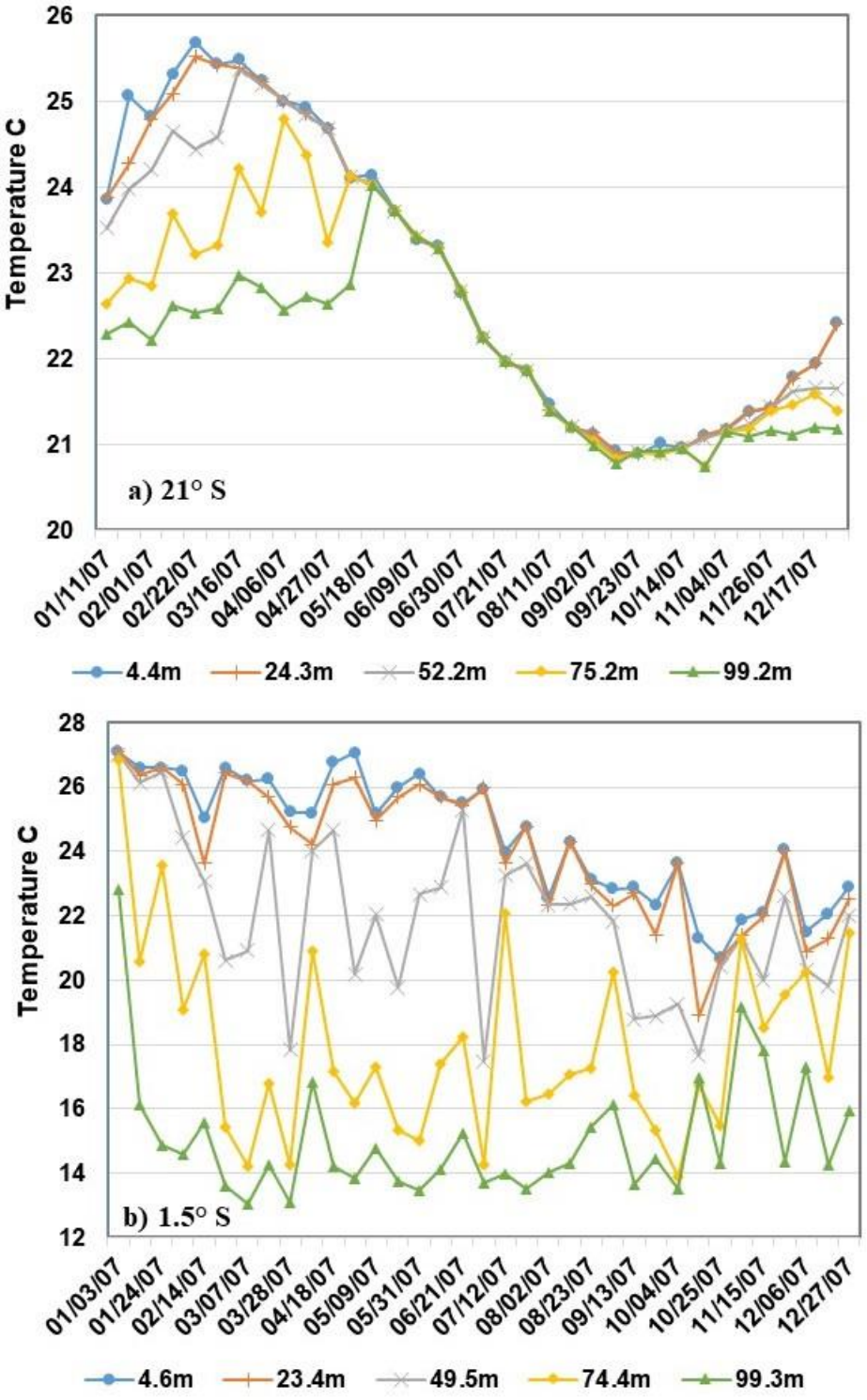

Figure 5: Argo float data for average latitudes of 21° and 1.5° S. At 21 S and higher latitudes, the solar heating and wind driven evaporation interact to produce a stable subsurface thermal gradient in the summer that is removed by excess cooling during the winter. Near the equator, the solar heating exceeds the evaporation in the eastern Pacific Ocean leading to the formation of the equatorial warm pool.

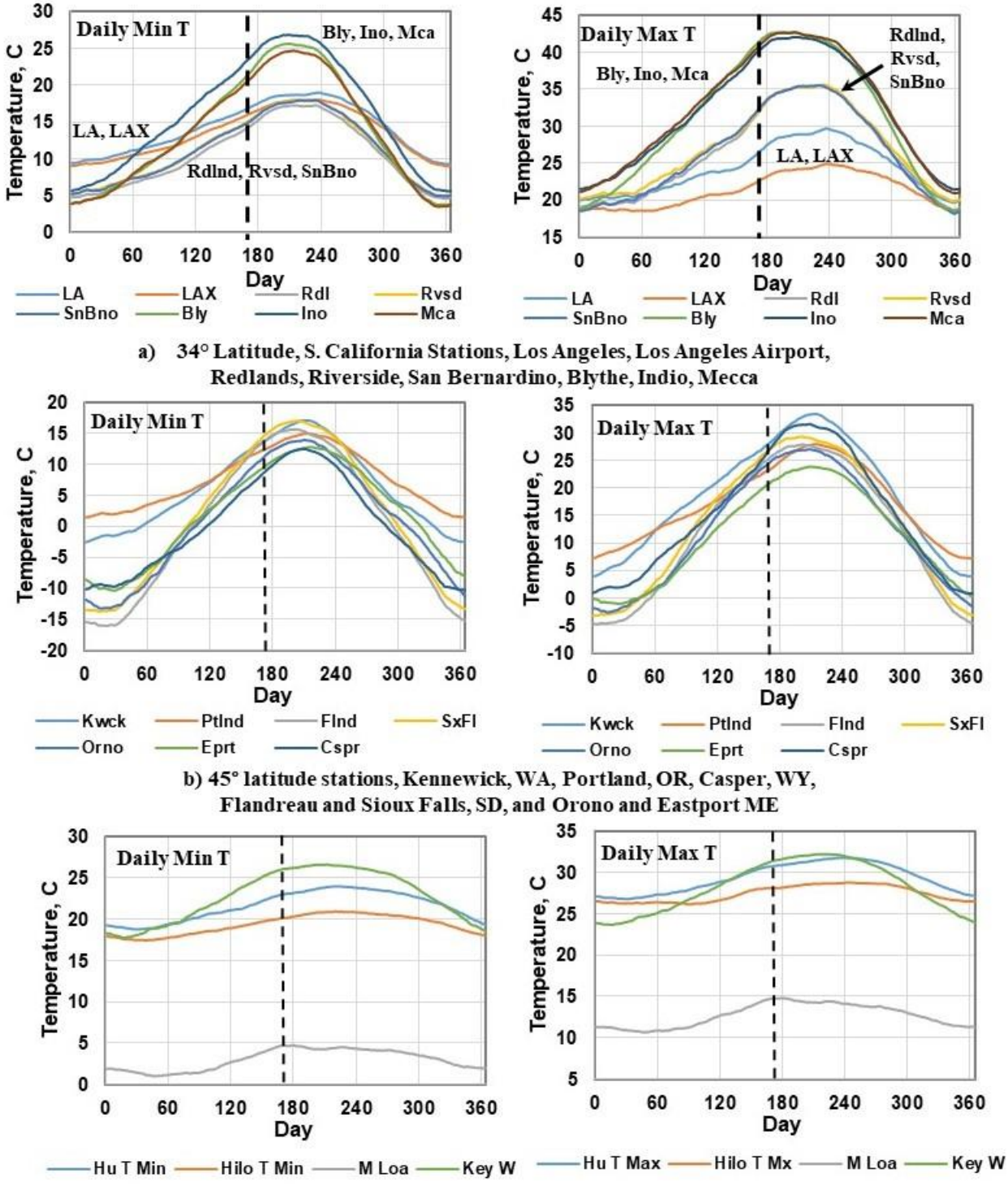

a) 34° Latitude, S. California Stations, Los Angeles, Los Angeles Airport, Redlands, Riverside, San Bernardino, Blythe, Indio, Mecca

b) 45° latitude stations, Kennewick, WA, Portland, OR, Casper, WY, Flandreau and Sioux Falls, SD, and Orono and Eastport ME

c) 20° latitude stations, Honolulu, HI, Hilo, HI, Mauna Loa, HI and Key West, FL.

Figure 6: 30 year minimum and maximum daily average temperatures for selected weather stations at 34°, 45° and 20° latitudes. The dotted lines indicated the peak solar flux at summer solstice. The seasonal phase shifts can be seen in the peak temperatures after solstice.

Over the last 200 years, the atmospheric concentration of CO_2 has increased by 120 ppm from 280 to 400 ppm. This has produced an increase in the downward LWIR flux at the surface of approximately 2 W m^{-2}. When this increase is added to the time dependent flux terms and coupled to the land and ocean thermal reservoirs, the increase in surface temperature is too small to measure. The observed changes in temperature in the climate record can be explained in terms of ocean oscillations superimposed on a temperature recovery from the Maunder minimum [Clark, 2019b; Akasofu, 2010].

Based on this discussion, a completely different approach to the analysis of surface temperature is needed. The current practice of averaging the minimum and maximum MSAT should be eliminated and the minimum MSAT and the delta T should be analyzed separately using realistic surface energy transfer terms. The idea of a 'one size fits all' climate model simulation in terms of latitude and longitude bins should be abandoned. The models should be configured to calculate the local weather station records, including any bias terms and location change. Climate models should include simulations of the ocean oscillations and the coupling of these to the weather station measurements. Concepts such as an equilibrium average climate state, radiative forcing and a climate sensitivity constant have no basis in the physical reality of dynamically coupled thermal reservoirs. These concepts belong in the same historical category of failed hypotheses as caloric, phlogiston and the luminiferous aether.

References

Akasofu, S-I, Natural Science **2**(11) 1211-1224 (2010), 'On the recovery from the Little Ice Age' http://www.scirp.org/Journal/PaperInformation.aspx?paperID=3217&JournalID=69

Andrews, R., 2017a, Energy Matters Sept 14 2017, 'Adjusting Measurements to Match the Models – Part 3: Lower Troposphere Satellite Temperatures', http://euanmearns.com/adjusting-measurements-to-match-the-models-part-3-lower-troposphere-satellite-temperatures/#more-19464

Andrews, R., 2017b, Energy Matters Aug 2 2017, 'Making the Measurements Match the Models – Part 2: Sea Surface Temperatures', http://euanmearns.com/making-the-measurements-match-the-models-part-2-sea-surface-temperatures/

Andrews, R., 2017c, Energy Matters July 27 2017, 'Adjusting Measurements to Match the Models – Part 1: Surface Air Temperatures', http://euanmearns.com/adjusting-measurements-to-match-the-models-part-1-surface-air-temperatures/

Clark, R. 2019a, '*A Dynamic Coupled Thermal Reservoir Approach to Atmospheric Energy Transfer Part III: The surface Temperature*', Ventura Photonics Monograph, VPM 004.1, Thousand Oaks, CA, May 2019

http://venturaphotonics.com/files/CoupledThermalReservoir_Part_III_Surface_Temperature.pdf

Clark, R. 2019b, '*A Dynamic Coupled Thermal Reservoir Approach to Atmospheric Energy Transfer Part IV: The Null Hypothesis for CO_2*' Ventura Photonics Monograph, VPM 005.1, Thousand Oaks, CA, May 2019

http://venturaphotonics.com/files/CoupledThermalReservoir_Part_IV_The_Null_Hypothesis.pdf

Clark, R. 2019c, '*A Dynamic Coupled Thermal Reservoir Approach to Atmospheric Energy Transfer Part V: Summary*', Ventura Photonics Monograph, VPM 006, Thousand Oaks, CA, May 2019

http://venturaphotonics.com/files/CoupledThermalReservoir_Part_V_Summary.pdf

Clark, R. 2019d, '*The Greenhouse Effect*', Ventura Photonics Monograph, VPM 003.2, Thousand Oaks, CA, May 2019

http://venturaphotonics.com/files/The_Greenhouse_Effect.pdf

Clark, R. 2019e, '*50 Years of Climate Fraud*', Ventura Photonics Monograph, VPM 002.1, Thousand Oaks, CA, May 2019

http://venturaphotonics.com/files/50_Years_of_Climate_Fraud.pdf

Clark, R., 2013a, Energy and Environment **24**(3, 4) 319-340 (2013), 'A dynamic coupled thermal reservoir approach to atmospheric energy transfer Part I: Concepts'

http://venturaphotonics.com/files/CoupledThermalReservoir_Part_I_E_EDraft.pdf

Clark, R., 2013b, Energy and Environment **24**(3, 4) 341-359 (2013) 'A dynamic coupled thermal reservoir approach to atmospheric energy transfer Part II: Applications'

http://venturaphotonics.com/files/CoupledThermalReservoir_Part_II__E_EDraft.pdf

D'Aleo, J. '*Progressive Enhancement of Global Temperature Trends*', Science and Public Policy Institute, July 2010. http://scienceandpublicpolicy.org/science-papers/originals/progressive-enhancement

Fourier, B. J. B.; Mem. R. Sci. Inst., (7) 527-604 (1827), 'Memoire sur les temperatures du globe terrestre et des espaces planetaires'

Hansen, J. et al, (45 authors), J. Geophys. Research **110** D18104 1-45 (2005) 'Efficacy of climate forcings' http://pubs.giss.nasa.gov/abs/ha01110v.html

Hansen, J.; D. Johnson, A. Lacis, S. Lebedeff, P. Lee, D. Rind and G. Russell Science **213** 957-956 (1981), 'Climate impact of increasing carbon dioxide'

IPCC, 2013: *Climate Change 2013: The Physical Science Basis. Contribution of Working Group I to the Fifth Assessment Report of the Intergovernmental Panel on Climate Change* Chapter 8 'Radiative Forcing' [Stocker, T.F., D. Qin, G.-K. Plattner, M. Tignor, S.K. Allen, J. Boschung, A. Nauels, Y. Xia, V. Bex and P.M. Midgley (eds.)]. Cambridge University Press, Cambridge, United Kingdom and New York, NY, USA, 1535 pp, doi:10.1017/CBO9781107415324.

http://www.climatechange2013.org/report/full-report/

Koll, D. D. B and T. W. Cronin., PNAS, www.PNAS.Org/Cgi/doi/10.1073/pnas.1809868115 pp. 1-6 (2018), 'Earth's outgoing longwave radiation linear due to H_2O greenhouse effect'.

Oke T. R., WMO/TD-No. 1250, World Meteorological Association, 2006, '*Initial guidance to obtain representative meteorological observations at urban sites*'